Robotica (2006) volume 24, pp. 31–37. © 2005 Cambridge University Press
doi:10.1017/S0263574704001237 Printed in the United Kingdom

Development of a biped walking robot actuated by a closed-chain mechanism

Hyeung-Sik Choi* and Yong-Heon Park

Division of Mechanical and Information Engineering, Korea Maritime University, Dongsam-Dong, Yeongdo-Ku, Pusan (South Korea)

(Received in Final Form: November 3, 2004)

SUMMARY

We developed a new type of a human-sized BWR (biped walking robot) driven by the closed-chain type of a joint actuator. Each leg of the BWR is composed of three pitch joints and one roll joint. In all, a 12 degree-of-freedom robot, including four arm joints, was developed. The BWR was designed to walk autonomously; it is actuated by small 90W DC motors/drivers and is has DC batteries and controllers. A new type of the joint actuator for the BWR is composed of the four-bar-link mechanism driven by a ball screw which has high strength and high gear ratio despite its light weight.

In this paper, analyses on the four-bar-link mechanism applied to the joint actuator and on the structure of the BWR are presented. Through walking experiments of the BWR, the superior trajectory-tracking ability of the proposed joint actuator is validated.

KEYWORDS: Biped walking robot; Ball screw; Four-bar-link mechanism.

I. INTRODUCTION

Since Vukobratovic and Stepanenko[1] have suggested a model of a BWR (biped walking robot), many people have conducted researches on BWRs. In the early stage of the research on BWRs, theoretical modeling and control of robot legs without balancing joints were performed by Gubina.[2] One of roles of BWRs is to serve or to cooperate with human beings in various environments. To walk in these conditions, the walking mode, such as the period of walk, step width and walking direction, should be changeable. However, BWRs composed of legs without balancing joints lack stability and walking ability. To improve the walking motion, research on modeling and control of BWRs with balancing joints was performed by Yamaguchi,[3] Lim[4] and Tzafestas.[5]

Since BWRs have many degrees of freedom, their dynamics are very complex. Theoretical modeling for actual gaits of BWRs is quite difficult. For supporting the heavy trunk and gaits of BWRs, it is more realistic to design and construct a strong actuating mechanism for leg joints.

As an early stage of the research on the driving mechanism, a hydraulic power system was applied to drive legs of the BWR by Takanish.[6] However, since the hydraulic system was so heavy, bulky and difficult to maintain, servo motors with a speed reducer have been most widely used to drive leg joints. The harmonic drive is the most widely used speed reducer since its gear ratio is so high and compact despite its light weight. But, despite the high gear ratio, it is not stiff enough to actuate leg joints of BWRs. To compensate for the gravity and the increased driving torque, a spring mechanism was devised and applied to leg joints by Yamaguchi.[7] Despite these approaches, the driving torque was not improved enough to actuate the BWRs. A biped robot aiming at having anthropomorphic characteristics was developed by Espiau,[8] whose joints are actuated by the rod crank system composed of screw nuts. Despite of a new actuator design, the capacity of the actuating AC motors/drivers is too big so that it might be quite difficult to walk autonomously. One of successful ways in developing human-sized BWRs is to devise actuators which are small and light but have high stiffness and high gear ratio.

Without strong joint actuators, the BWR has very limited walking ability. Shih[9] developed a small BWR which 800(mm) high and seven D.O.F.s, include one prismatic balancing joint. In 1998, Yamaguchi[7] developed a small nine D.O.F.s BWR which is 1405(mm) high and had a 0.12(m/sec) walking speed. So far, the most developed human-sized BWRs are the Asimo and P3 robots. The P3 BWR was developed by Hirai[10] at the Honda company Ltd., and a smaller but improved version is Asimo. They are developed as humanoids, and walk like human beings. The speed reducer for leg joints is specified as the harmonic drive, but the information on the driving mechanism, such as the capacity of actuating motors, details of the speed reducers, and control algorithm, is not yet available.

We developed a 12 D.O.F.s lower part of a human-sized BWR, which is actuated by a novel joint actuator using the four bar links driven by the ball screw. We present the structure, the actuating mechanism, the composed controller and driver, and the walking performance of the BWR. In section 2 of the paper, a four-bar-link mechanism actuated by the ball screw is analyzed. In section 3, the kinematic mechanism of the BWR actuated by the proposed joint actuators is shown. In addition to this, the mechanical structure and control systems, including the motor driver and motion control system, are presented in section 4. Finally, through walking tests of the actuator and the BWR, performance results are shown and discussed.

* Corresponding author. E-mail: hchoi@mail.hhu.ac.kr

https://doi.org/10.1017/S0263574704001237 Published online by Cambridge University Press

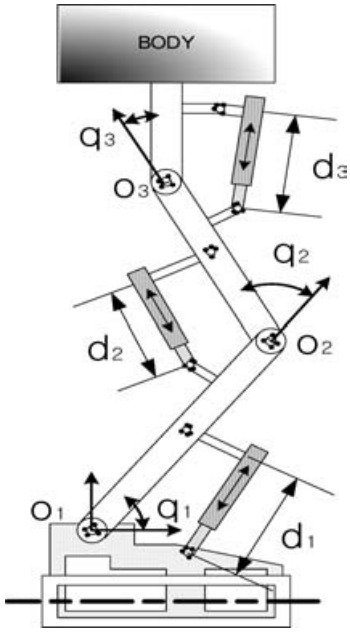


Fig. 1. Structure of one leg.



Fig. 2. Four-bar-link mechanism actuated by ball screw.

II. MECHANISM OF THE JOINT ACTUATORS

We developed the lower body of the humanoid robot, which has two legs and a trunk, and two arms. Each leg has a pelvis, knee and two ankle joints. The leg joints of the BWR moving along the pitch direction are composed of an ankle, knee and pelvis joints, as shown in Fig. 1. The joint actuators are composed of the four-bar-link mechanism whose one link is the ball screw actuator, as shown in Fig. 2.

II.1. Four-bar-link mechanism for the ankle joint

The ankle joint is a part of the four-bar-link mechanism, which is rotated by driving the ball screw along the translational direction. The structure of the four-bar link mechanism is shown in Fig. 3, where b_1 represents a connecting bar between the ankle joint and the knee joint, and c_1 represents another bar composed of the foot. The ankle joint β_1 rotates as the position of the ball screw d_1 moves in the translational direction. The relation between the ankle

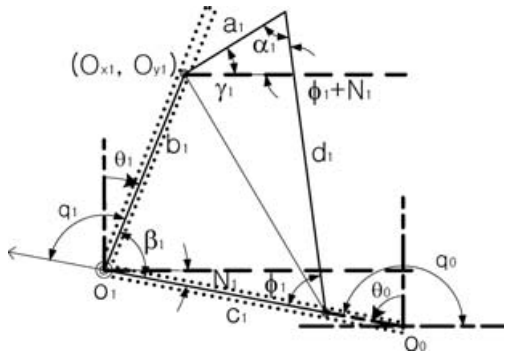


Fig. 3. Geometric configuration of the ankle joint.

joint and the position of the ball screw can be expressed by a trigonometric function. As shown in Fig. 3, the rectangle is divided into two triangles, and the Cosine rule in the trigonometric function is applied to both triangles to find the relation between β_1 and d_1. The equation showing the relation is expressed as

$$d_1^2 = A_1 + B_1 \cos\beta_1 + C_1 d_1 \tag{1}$$

where

$$A_1 = b_1^2 + c_1^2 - a_1^2,$$
$$B_1 = -2b_1c_1,$$
$$C_1 = 2a_1 \cos\alpha_1$$

where the length of links a_1, b_1, c_1, and the angles α_1 and N_1 are design parameters and all known. Solving Eq. (1) with respect to the displacement of the ball screw d_1 yields

$$d_1 = \frac{C_1 + \left[C_1^2 + 4(A_1 + B_1\cos\beta_1)\right]^{0.5}}{2} \tag{2}$$

By differentiating d_1 with respect to time, the kinematic relation is obtained as

$$\dot{d}_1 = -\left[C_1^2 + 4(A_1 + B_1\cos\beta_1)\right]^{-0.5} B_1 \sin\beta_1 \dot{\beta}_1 \tag{3}$$

Using the relation $q_1 = \pi - \beta_1$, the kinematic relation between $\dot{q}_1$ and $\dot{\beta}_1$ is expressed as

$$\dot{\beta}_1 = \dot{q}_1 = R_{11} = \frac{\left[C_1^2 + 4(A_1 + B_1\cos\beta_1)\right]^{0.5}}{B_1 \sin\beta_1}\dot{d}_1 \tag{4}$$

II.2. Four-bar-link mechanism for the knee joint

The four-bar-link mechanism applied to the knee joint is shown in Fig. 4, where b_2 represents a connecting bar between the knee joint and the pelvis joint, and d_2 represents the translational displacement of the ball screw. The relation is shown between d_2 and β_2 which is the revolution joint of the knee as

$$d_2 = \frac{C_2 + \left[C_2^2 + 4\,(A_2 + B_2\cos\beta_2)\right]^{0.5}}{2} \tag{5}$$

https://doi.org/10.1017/S0263574704001237 Published online by Cambridge University Press

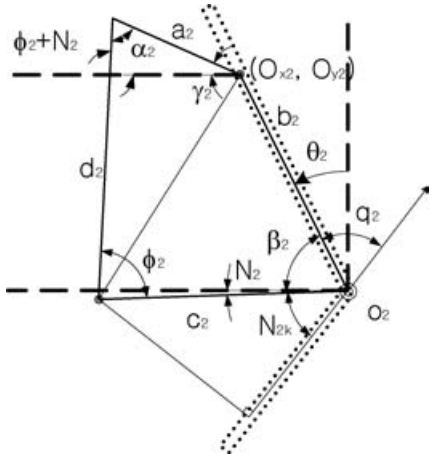


Fig. 4. Geometric configuration of the knee joint.

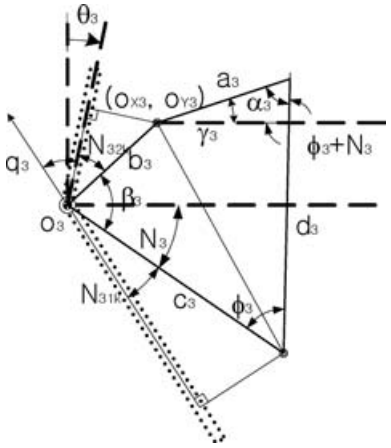


Fig. 5. Geometric configuration of the pelvis joint.

where

$$A_2 = b_2^2 + c_2^2 - a_2^2,$$
$$B_2 = -2b_2c_2,$$
$$C_2 = 2a_2 \cos\alpha_2$$

where the length of links a_2, b_2, c_2, and the angles a_2 and N_{2k} are all known design parameters. As shown in Fig. 4, the relating equation between q_2 and d_2 is obtained as

$$\dot{d}_2 = -\left[C_2^2 + 4(A_2 + B_2\cos\beta_2)\right]^{-0.5} B_2 \sin\beta_2\dot{\beta}_2 \qquad (6)$$

Also, using relation $q_2 = \pi - \beta_2 - N_{2k}$, the kinematic relation between $\dot{\beta}_2$ and $\dot{d}_2$ is obtained as

$$\dot{\beta}_2 = -\dot{q}_2 = R_{12} = \frac{\left[C_2^2 + 4(A_2 + B_2\cos\beta_2)\right]^{0.5}}{B_2\sin\beta_2}\dot{d}_2. \qquad (7)$$

II.3. Four-bar-link mechanism for the pelvis joint

The four-bar-link mechanism applied to the pelvis joint has the similar structure as those of the ankle and knee joints, which is shown in Fig. 5, where the length of links a_3, b_3, c_3, and the angles α_3, N_{31k}, and N_{32k} are all known and constant. N_3 is a dependent angle upon the joint angles of the knee and pelvis. d_3 represents the translational displacement of the ball screw. The joint angle β_3 is determined using the Cosine Rule in the trigonometric function as follows:

$$d_3 = \frac{C_3 + \left[C_3^2 + 4(A_3 + B_3\cos\beta_3)\right]^{0.5}}{2} \qquad (8)$$

where $A_3 = b_3^2 + c_3^2 - a_3^2$, $B_3 = -2b_3c_3$, and $C_3 = 2a_3\cos\alpha_3$.

Also, the relation between d_3 and β_3 which is the revolution joint of the pelvis is expressed as

$$q_3 = \pi - \beta_3 - N_{31k} - N_{31k} \qquad (9)$$

The relations between q_3, $\dot{q}_3$ and d_3, $\dot{d}_3$ are similarly obtained as those of the ankle and knee.

III. THE DESCRIPTION OF THE ROBOT

The structure of the developed BWR is analyzed in this section.

III.1. The structure of BWR

The BWR is shown in Fig. 6, and its structure is composed of

- Six leg joints actuated by the four-bar-link mechanism
- Two roll joints for ankles actuated by the motors attached with the speed reducers
- Four arm joints actuated by motors attached with the speed reducers.

The six joints for legs are designed for pitching motion, and the two joints for ankles are designed for balancing the weight of the robot in the roll direction. The arms were designed to perform manual operations and to help balancing the pitching motion during walking motion.

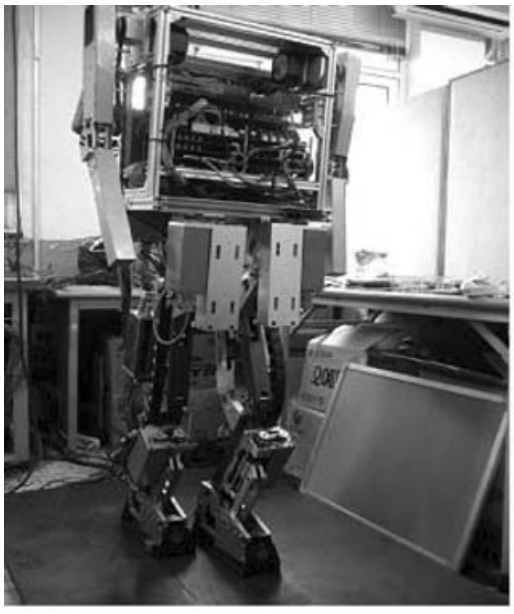


Fig. 6. 12 D.O.F BWR.

https://doi.org/10.1017/S0263574704001237 Published online by Cambridge University Press

Table I. Specification of the KUBIR actuators.

	Parts					
	Right and Left Legs				Balancing Weight	
Item	foot (Roll)	ankel	knee	pelvis	Pitch	Roll
DC Servo Motor[W]	90	90	90	90	90	90
Gear Ratio	216:1	1:1	1:1	1:1	126:1	126:1
Encoder Resolution	2000	2000	2000	2000	2000	2000
Lead of Ball Screw(mm/rev)		5	5	5		

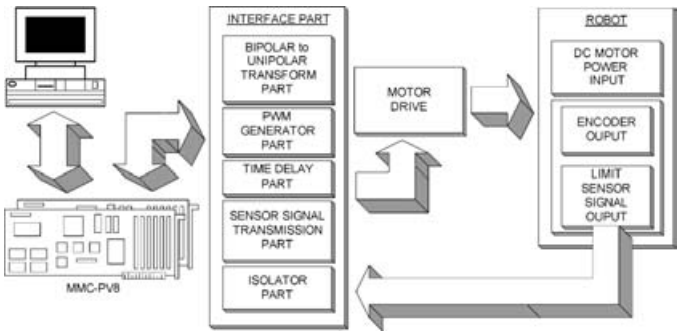


Fig. 7. Block diagram of the total control system.

The height of KUBIR is 1450(mm). The motor to actuate the ball screw of the four-bar-link is a DC motor with an incremental encoder. The specification of the actuation motors and ball screws for the BWR is shown in Table I.

IV. CONTROL SYSTEM

The BWR was designed for autonomous walking such that it is boarded with the embeded controller, driver, and batteries. To reduce the weight of the robot, we used small 90W DC motors as driving motors for the four-bar-link joint actuator, and we also developed DC motor drivers and I/O(input-output) interface system. We constructed the whole control system except the motion control board in order to reduce the size of the control system. The structure of the developed control system is shown in Fig. 7 and its picture is shown in Fig. 8. The constructed system consists of the following parts:

- DC servo motor driver
- Commercial motion controller (MMC-PV8)
- Main control system
- System I/O interface.

To reduce the size and weight of robot, we constructed the motor driver by using FET power devices and related electronic devices. The driver can supply the power to rotate the motor in a bi-direction and has the capability of limiting over-current flow to protect the motors by employing Hall sensors.

The robot has twelve joints composed of eight leg joints and four arm joints. All the joints are designed

Table II. Specification of MMC-PV8 controller.

Item	Specification
CPU	TMS320C31
Sampling Rate	1 msec
Analog ourput	±10V, 12 bit resolution
Analog input	4 channel, 12 bit resolution
User I/O	TTL Level, 32 channel
System I/O	16 channel

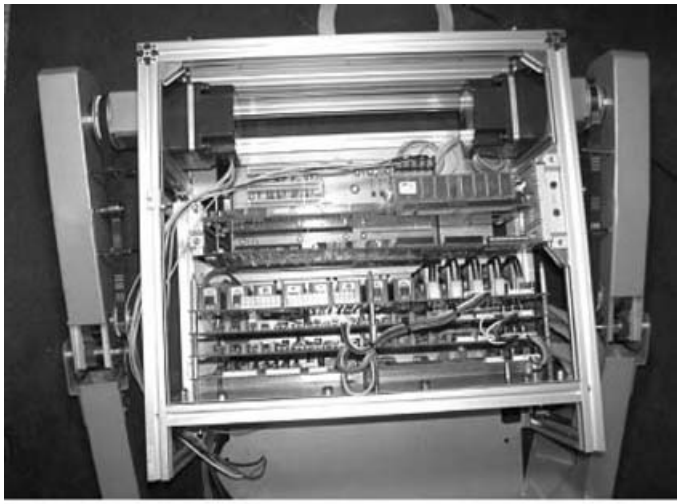


Fig. 8. The controller of the BWR.

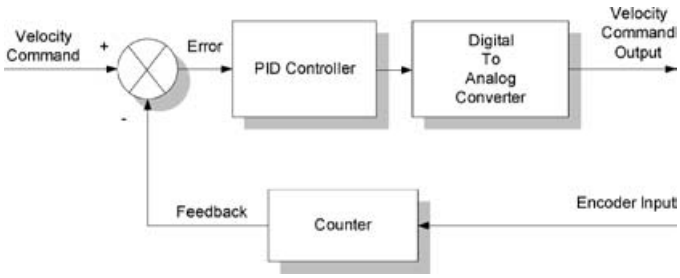


Fig. 9. Control structure of MMC.

to be active joints such that the robot requires twelve actuators composed of motors and drivers. To control them, a two motion controllers named MMC(multi-motion control) board whose control structure as shown in Fig. 9 was used. The board has a DSP processor which can mak ehigh speed calculation and has a PIDF (Proportional-Integral-Derivative-FeedforWard) control loop. Detailed informations is specified in Table II, and the control input algorithm consists of

$$Y_{vn} = K_R[K_{DP} \times PE_n + K_{DI} \times PS_n + K_{DD} \times (PE_n - PE_{n-1}) + K_{DF} \times V_n]$$

where

Y_{vn}: PID and Feedforward control input

K_R: Scale Factor (9 bit resolution)

n: Sample Period

K_{DP}, K_{DI}, K_{DD}, K_{DF}: Proportional, Integral, Derivative, Feedforward gain

https://doi.org/10.1017/S0263574704001237 Published online by Cambridge University Press



Fig. 10. The motion capture system.

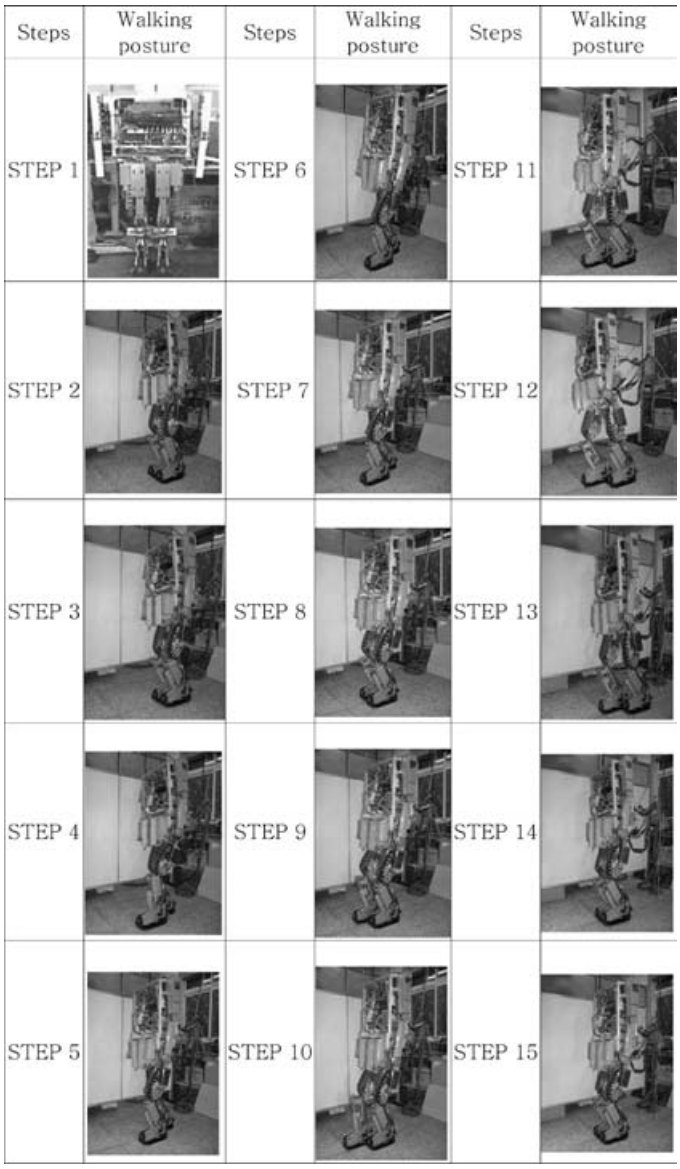


Fig. 11. Walking motion of the developed BWR.

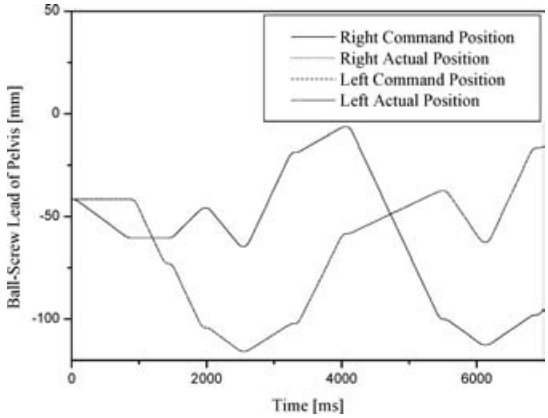


Fig. 12. Walking path of pelvice joint.

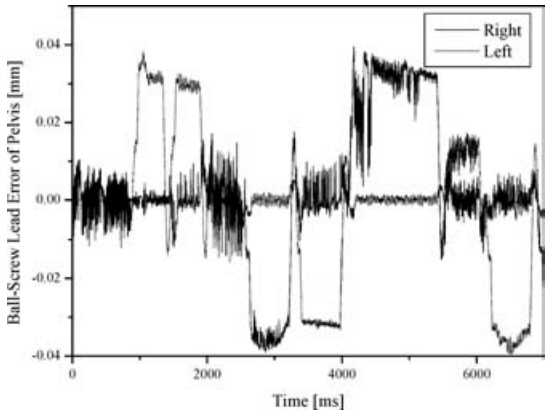


Fig. 13. Tracking error of pelvise joint.

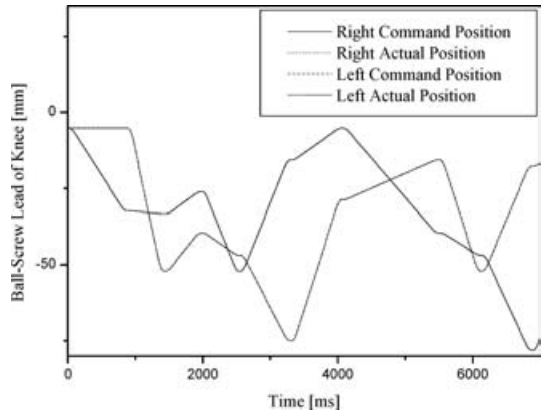


Fig. 14. Path tracking of knee joint.

PS_n: sum of position errors (PE_n)
PE_n: position error during sample period
V: velocity input during sample period.

As a main control system for the biped, we used the Pentium IV on-board computer which contains the MMC motion controller. The main control system edits control programs, gain setting of the PIDF control algorithm in the motion controller, planning of joint trajectories, and monitoring the motion of the robot.

For the communication between the MMC board, the motor and drivers, we constructed an I/O interface system. The structure is shown in Fig. 7 and Fig. 8, where the

https://doi.org/10.1017/S0263574704001237 Published online by Cambridge University Press

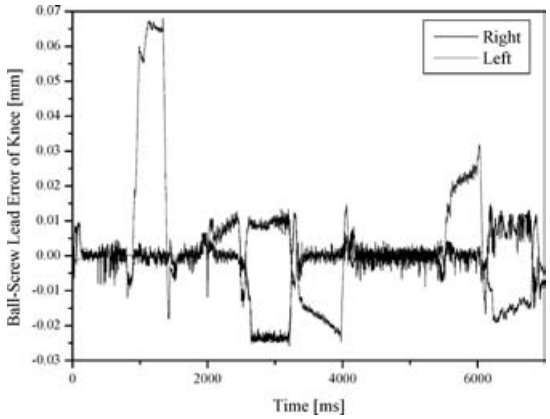


Fig. 15. Tracking error of knee joint.

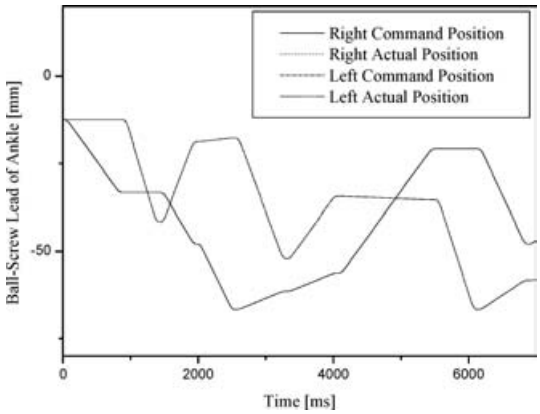


Fig. 16. Path tracking of ankle joint.

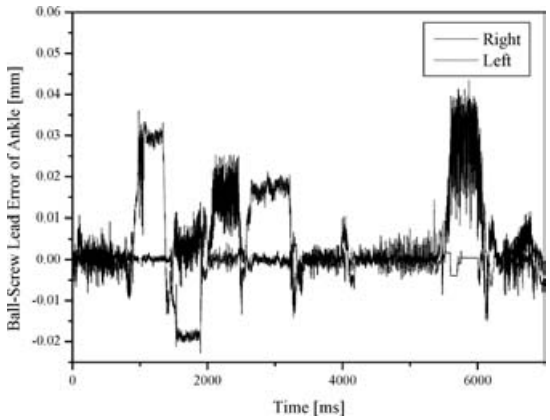


Fig. 17. Tracking error of ankle joint.

bipolar-to-unipolar transform part generates the velocity and direction signal for the motor. The pulse width modulation (PWM) generator part creates the PWM signal. The I/O interface system includes a time delay circuit and a photo-isolator circuit. The time delay circuit protects the driver circuit devices from over-current flows by delaying the input over-current flow for a short time for a bi-directional power change. The photo-isolator circuit filters out noises and cuts off high reverse currents. In the I/O interface system, the sensor signal transmission circuit transfers encoder and limit sensor signals to the motion controller.

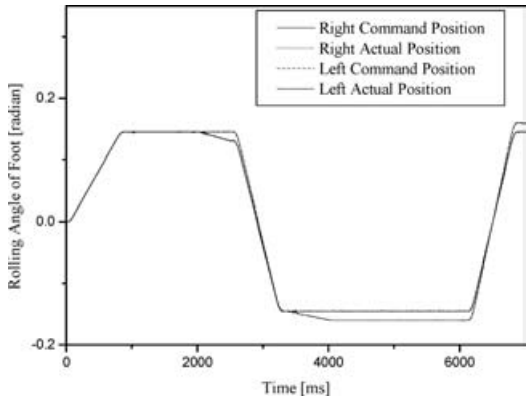


Fig. 18. Path tracking of ankle roll joint.

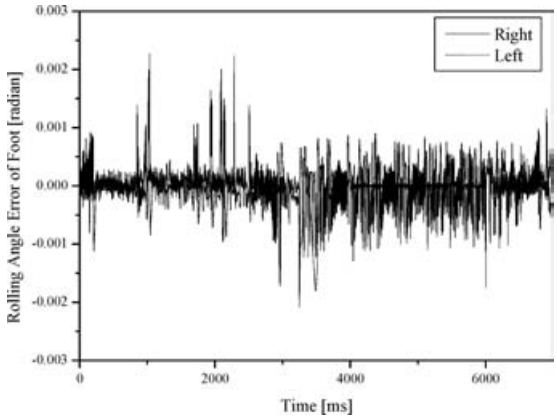


Fig. 19. Tracking error of ankle roll joint.

V. PERFORMANCE TESTS

The height of our BWR is 1450(mm). It weighs 70 Kg and has eight joints in legs and four arm joints. A four-bar-link actuator was developed to actuate the joint of the BWR and was applied to six pitching leg joints. For arm joints, DC motors with a speed reducer were applied.

We performed walking tests of the BWR where reference data for the walking joint trajectories were obtained from the data of the human walking motion, using the motion capture system. To obtain reference walking data, an assistant wears the motion capture system composed of eight joints with rotary potentiometers, as shown in Fig. 10. The reference walking data were partially exploited as input data. For one period walking, a number of reference tracking joint angles were given. One period of walking motion is shown in Fig. 11. A slow walking test was performed such that one period of walking motion for both legs took 7 seconds, and the gait width was 50 cm. As shown in Fig. 11, the BWR could successfully walk along the specified trajectory.

One of the important purposes of the test was to identify the tracking ability of the joint actuator weighing 70 Kg, using the developed small-sized joint actuators. Figs. 12–19 show the trajectory tracking of ball screws along desired trajectories. Figs. 13, 15, 17 and 19 show trajectory tracking errors of all the joints. As shown in the

https://doi.org/10.1017/S0263574704001237 Published online by Cambridge University Press

figures, joint actuators show a good performance with small tracking errors. Throughout the test, all the system, including motor driver, I/O system and mechanical system, performed well.

The developed robot is not perfectly designed as anthropomorphic so that it cannot walk fast and stably enough as a human being does. However, despite this, the BWR showed stable walking ability. This shows that the proposed four-bar-link joint actuator of the robot shows the capability to actuate a heavy BWR by using a small 90W motor.

VI. CONCLUSION

We developed a 12 D.O.F.s lower part of the BWR which is actuated by a new joint actuator composed of a four-bar-link mechanism. The weight of the BWR is 70 Kg and the height is 1450 mm. The whole mechanical and electronic system was built except the motion controller. According to walking performance tests, despite the small-powered actuating motors, the proposed joint actuators could successfully drive the heavy robot along the specified trajectory. This shows that the proposed actuator has enough stiffness and torque transmission ability. Through the basic walking tests, we obtained experimental data of the stable walking motion of the BWR, and found that the proposed actuator has high transmission ability and that the BWR, including the proposed actuator, has a capability of carrying a heavier weight and of a faster walking motion.

Grant sponsor: Korea Research Foundation, grant number: KRF-2003-002-000024.

References

1. M. Vukobratovic and M. Stepanenko, "Mathematical models of general anthropomorphic systems", *Mathematical Biosciences* **17**, 191–242 (1973).
2. F. Gubina, H. Hemami and R. B. McGhee, "On the dynamic stability of biped locomotion", *IEEE Trans. on Biomd. Engineering*, **BME-21**, 102–108 (1974).
3. J. Yamaguchi et al, "Development of a biped walking robot compensating for three-axis moment by trunk motion", *IEEE/RSJ Int. Conf. on Intelligent Robots and System* (1993) pp. 561–566.
4. S. H. Lim, "*A study on the implementation of zero moment point control for IWR-III biped walking robot*", *Ph.D. Dissertation* (Inha University, 1999).
5. S. G. Tzafestas, R. E. Krikochoritis and C. S. Tzafestas, "Robust-Adaptive Gait Control of a 9-Link Biped Robot", *Syst. Anal. Modelling Simul.* **31**(4) 247–304 (1998).
6. A. Takanishi, M. Ishida, Y. Yamazaki and I. Kato, "The Realization of Dynamic Walking by The Biped Walking Robot WL-10RD", *Journal of the Robotics Society of Japan* **3**(4) 325–336 (1985).
7. J. Yamaguchi, D. Nishino and A. Nakanishi, "Realization of Dynamic Biped Walking Varying Joint Stiffness Using Antagonistic Driven Joints", *IEEE Int. Conf. on Robotics and Automation* 2022–2029 (1998).
8. B. Espiau and P. Sardain, "The anthropormophic biped robot BIP2000", *Proc. IEEE Int. Conf. on Robotics and Automation* (2000) pp. 3996–4001.
9. C. Shih, "Analysis of the dynamics of a biped robot with seven degrees of freedom", *Proc. IEEE Int. Conf. on Robotics and Automation* (1996) pp. 3008–3013.
10. K. Hirai, M. Hirose, Y. Haidawa and T. Takenaka, "The development of honda humanoid robot", *Proc. IEEE International Conf. on Robotics and Automation* (1998) pp. 1321–1326.

https://doi.org/10.1017/S0263574704001237 Published online by Cambridge University Press